

Unprecedented 4- and 6-Connected 2D Coordination Networks Based on 4⁴-Subnet Tectons, Showing Unusual Supramolecular Motifs of Rotaxane and Helix

Lu-Fang Ma,[†] Li-Ya Wang,^{*†} Miao Du,^{*‡} and Stuart R. Batten[§]

[†]College of Chemistry and Chemical Engineering, Luoyang Normal University, Luoyang 471022, People's Republic of China, [‡]College of Chemistry and Life Science, Tianjin Key Laboratory of Structure and Performance for Functional Molecule, Tianjin Normal University, Tianjin 300387, People's Republic of China, and [§]School of Chemistry, Monash University, Victoria 3800, Australia

Received September 30, 2009

Two unprecedented 2D coordination polymers with 4- and 6-connected topological nets, arising from the different linkages of two adjacent 4⁴ layers, were prepared from Co^{II}, 1,3-bis(4-pyridyl)propane, and different isophthalate tectons.

The deliberate design and synthesis of supramolecular solids with desired crystalline architectures and properties is an ultimate goal of crystal engineering. One of the most fascinating aspects of this topic concerns the variety of topologies of the extended lattices.^{1–3} Net topology represents an important and essential problem of the construction and analysis of coordination frameworks, which has also

been the subject of several related studies, with fundamental contributions by Wells,⁴ Smith,⁵ and O'Keeffe and Hyde.⁶

Nodes of 3-, 4-, and 6-connectivity are of most relevance, and a variety of such uninodal net topologies have been realized by 3D coordination frameworks, for instance, **srs**, **dia**, **cds**, **nbo**, **pcu**, etc.⁷ Meanwhile, the simple 2D layers with relevant connectivity are usually constructed by the uniform and regular polygon (such as triangle, square, and hexagon), and their corresponding network symbols are designated as 6³, 4⁴, and 3⁶, respectively.⁸ However, other 4- and 6-connected layers have rarely been reported so far.⁹ Thus, the construction of new or unusual 4- and 6-connected 2D net topologies is of great interest at a current stage.

Our recent study on coordination assemblies using a flexible dipyridyl linker 1,3-bis(4-pyridyl)propane (bpp) and isophthalate derivatives states a reliable strategy for obtaining new topological prototypes of coordination nets.¹⁰ Also, a minor change of the isophthalate building blocks may be applied to realize good structural control of the resulting coordination polymers. Thus, these results promote us to further explore other new coordination frameworks with 5-methylisophthalate (H₂mip) and 5-*tert*-butylisophthalate (H₂tbip), which may serve as good candidates for the design of unique topological networks. Fortunately, the foregoing effort has led to the isolation of a pair of unique 4- and 6-connected 2D supramolecular architectures by the assembly of the bpp linker with Co^{II} and H₂mip or H₂tbip.

*To whom correspondence should be addressed. E-mail: wly@lynu.edu.cn (L.-Y.W.), dumiao@public.tpt.tj.cn (M.D.).

(1) (a) Batten, S. R.; Robson, R. *Angew. Chem., Int. Ed.* **1998**, *37*, 1460. (b) Carlucci, L.; Ciani, G.; Proserpio, D. M. *Coord. Chem. Rev.* **2003**, *246*, 247. (c) Tong, M. L.; Chen, X. L.; Batten, S. R. *J. Am. Chem. Soc.* **2003**, *125*, 16170. (d) Hargman, P. J.; Hargman, D.; Zubieta, J. *Angew. Chem., Int. Ed.* **1999**, *111*, 2798. (e) Moulton, B.; Zaworotko, M. J. *Coord. Chem. Rev.* **2001**, *101*, 1629. (f) Rao, C. N. R.; Natarajan, S.; Vaidhyanathan, R. *Angew. Chem., Int. Ed.* **2004**, *43*, 1466.

(2) (a) Du, M.; Zhang, Z. H.; Tang, L. F.; Wang, X. G.; Zhao, X. J.; Batten, S. R. *Chem.—Eur. J.* **2007**, *13*, 2578. (b) Du, M.; Zhao, X. J.; Guo, J. H.; Batten, S. R. *Chem. Commun.* **2005**, 4836. (c) Zheng, S. R.; Yang, Q. Y.; Liu, Y. R.; Zhang, J. Y.; Tong, Y. X.; Zhao, C. Y.; Su, C. Y. *Chem. Commun.* **2008**, 356. (d) Hong, S.; Zou, Y.; Moon, D.; Lah, M. S. *Chem. Commun.* **2007**, 1707. (e) Fang, Q. R.; Zhu, G. S.; Xue, M.; Sun, J. Y.; Wei, Y.; Qiu, S. L.; Xu, R. R. *Angew. Chem., Int. Ed.* **2005**, *44*, 3845. (f) Youm, K. T.; Kim, M. G.; Ko, J.; Jun, M. J. *Angew. Chem., Int. Ed.* **2006**, *45*, 4003.

(3) (a) Fang, Q. R.; Zhu, G. S.; Jin, Z.; Xue, M.; Wei, X.; Wang, D. J.; Qiu, S. L. *Angew. Chem., Int. Ed.* **2006**, *45*, 6126. (b) Li, J. R.; Yu, Q.; Sanudo, E. C.; Tao, Y.; Bu, X. H. *Chem. Commun.* **2007**, 2602. (c) Cheon, Y. E.; Suh, M. P. *Chem.—Eur. J.* **2008**, *14*, 3961. (d) Huang, Y. G.; Wu, B. L.; Yuan, D. Q.; Xu, Y. Q.; Jiang, F. L.; Hong, M. C. *Inorg. Chem.* **2007**, *46*, 1171. (e) Liu, C. M.; Gao, S.; Zhang, D. Q.; Zhu, D. B. *Cryst. Growth Des.* **2007**, *7*, 1312. (f) Wang, S. N.; Yang, Y.; Bai, J. F.; Li, Y. Z.; Scheer, M.; Pan, Y.; You, X. Z. *Chem. Commun.* **2007**, 4416. (g) Wang, X. L.; Qin, C.; Wang, E. B.; Li, Y. G.; Su, Z. M. *Chem. Commun.* **2005**, 5450.

(4) (a) Wells, A. F. *Structural Inorganic Chemistry*, 5th ed.; Oxford University Press: Oxford, U.K., 1984. (b) Wells, A. F. *Three-dimensional Nets and Polyhedra*; Wiley: New York, 1977.

(5) (a) Smith, J. V. *Chem. Rev.* **1988**, *88*, 149. (b) Smith, J. V. *Tetrahedral Frameworks of Zeolites, Clathrates and Related Materials*; Landolt-Bornstein New Series IV/14 Subvolume A; Springer: Berlin, 2000.

(6) (a) O'Keeffe, M.; Hyde, S. T. *Zeolites* **1997**, *19*, 370. (b) O'Keeffe, M.; Hyde, B. G. *Crystal Structures I: Patterns and Symmetry*; Mineralogical Society of America: Chantilly, VA, 1996. (c) O'Keeffe, M. Z. *Kristallogr.* **1991**, *196*, 21. (d) Ockwig, N. W.; Delgado-Friedrichs, O.; O'Keeffe, M.; Yaghi, O. M. *Acc. Chem. Res.* **2005**, *38*, 176.

(7) Reticular Chemistry Structure Resource (RCSR), <http://rcsr.anu.edu.au/>.

(8) (a) Hill, R. J.; Long, D.; Champness, N. R.; Hubberstey, P.; Schröder, M. *Acc. Chem. Res.* **2005**, *38*, 337. (b) Kim, H.; Park, G.; Kim, K. *CrystEngComm* **2008**, *10*, 954.

(9) (a) Hill, R. J.; Long, D. L.; Turvey, M. S.; Blake, A. J.; Champness, N. R.; Hubberstey, P.; Wilson, C.; Schröder, M. *Chem. Commun.* **2004**, 1792. (b) Sun, R.; Wang, S. N.; Xing, H.; Bai, J. F.; Li, Y. Z.; Pan, Y.; You, X. Z. *Inorg. Chem.* **2007**, *46*, 8451.

(10) Ma, L. F.; Wang, Y. Y.; Liu, J. Q.; Yang, G. P.; Du, M.; Wang, L. Y. *CrystEngComm* **2009**, *11*, 1800.

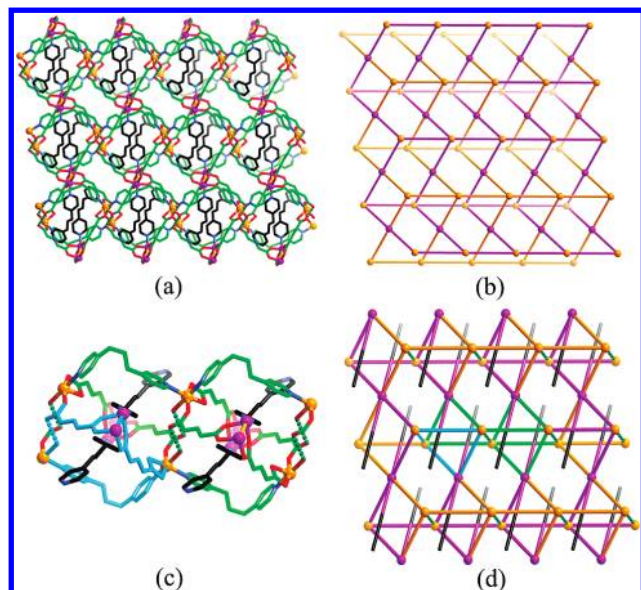


Figure 1. Views of **1**: (a) sheet structure; (b) schematic view of the 2D network topology. The purple spheres represent the Co1 dimeric nodes, and the orange balls represent the Co2 ions. (c) View of the rotaxane interactions highlighted with all of the non-H atoms added. (d) Schematic view of the 2D network with the monodentate bpp ligands as pendants.

Complexes **1** and **2** were obtained by solvothermal reactions of $\text{Co}(\text{OAc})_2 \cdot 4\text{H}_2\text{O}$, bpp, and KOH with H_2mip or H_2tbip ,^{11,12} which have been characterized by IR spectra, elemental analysis, and powder X-ray diffraction (PXRD) patterns (see Figure S1 in the Supporting Information).

Complex **1** contains two types of Co^{II} centers, two types of mip ligands, two types of bpp linkers (one monodentate and one bridging), and one aqua ligand (see Figure S2 in the Supporting Information). The Co1 ions are bridged to give a dimer by four carboxylate groups from four different mip ligands (two of each type). Each Co1 ion also coordinates to a monodentate bpp ligand, affording a square-pyramidal sphere. The four mip ligands radiating out from the dimer then coordinate to the Co2 atoms. One type of mip bonds in a unidentate fashion to Co2, while the other is chelated to the second metal center. Each octahedral Co2 is, in turn, coordinated to one chelated carboxylate, one unidentate

(11) Preparation of $[\text{Co}_2(\text{mip})_2(\text{bpp})_2(\text{H}_2\text{O})]_n$ (**1**). A mixture of H_2mip (35.2 mg, 0.2 mmol), bpp (40.4 mg, 0.2 mmol), $\text{Co}(\text{OAc})_2 \cdot 4\text{H}_2\text{O}$ (48.0 mg, 0.2 mmol), KOH (11.2 mg, 0.2 mmol), and H_2O (15 mL) was placed in a Teflon-lined stainless steel vessel, heated to 180 °C for 4 days, and then cooled to room temperature over 1 day. Red block crystals of **1** were obtained in 36% yield (32 mg). Anal. Calcd for $\text{C}_{44}\text{H}_{42}\text{Co}_2\text{N}_4\text{O}_9$: C, 59.47; H, 4.76; N, 6.30. Found: C, 59.53; H, 4.82; N, 6.24. IR (cm^{-1}): 3058 m, 1615 s, 1583 m, 1547 m, 1425 s, 1387 s, 1223 m, 777 s, 726 m. Preparation of $[\text{Co}_2(\text{tbip})_2(\text{H}_2\text{tbip})(\text{bpp})(\text{H}_2\text{O})]_n$ (**2**). The same synthetic method as that for **1** was used except that H_2mip was replaced by H_2tbip . Red block single crystals of **2** were obtained in 39% yield (39 mg). Anal. Calcd for $\text{C}_{49}\text{H}_{54}\text{Co}_2\text{N}_5\text{O}_{13}$: C, 59.04; H, 5.46; N, 2.81. Found: C, 59.01; H, 5.51; N, 2.91. IR (cm^{-1}): 2966 m, 1687 s, 1625 s, 1583 m, 1433 m, 1383 s, 1282 s, 1018 m, 911 m, 760 m, 711 m.

(12) Crystal data for **1**: $\text{C}_{44}\text{H}_{42}\text{Co}_2\text{N}_4\text{O}_9$ ($M_r = 888.68$), triclinic, $P\bar{1}$, $a = 11.392(3)$ Å, $b = 12.864(3)$ Å, $c = 15.790(4)$ Å, $\alpha = 106.490(2)^\circ$, $\beta = 102.053(2)^\circ$, $\gamma = 97.252(2)^\circ$, $V = 2127.1(9)$ Å³, $Z = 2$, $\rho = 1.387$ g cm⁻³, $\mu = 0.839$ mm⁻¹, $S = 1.043$, $R = 0.0409$ and $wR = 0.1205$ [$I > 2\sigma(I)$], and $R = 0.0488$ and $wR = 0.1281$ (all data). CCDC number: 740347. Crystal data for **2**: $\text{C}_{49}\text{H}_{54}\text{Co}_2\text{N}_5\text{O}_{13}$ ($M_r = 996.80$), monoclinic, $C2/c$, $a = 21.974(3)$ Å, $b = 31.948(4)$ Å, $c = 14.1566(19)$ Å, $\beta = 97.099(2)^\circ$, $V = 9862(2)$ Å³, $Z = 8$, $\rho = 1.343$ g cm⁻³, $\mu = 0.736$ mm⁻¹, $S = 1.042$, $R = 0.0909$ and $wR = 0.2432$ [$I > 2\sigma(I)$], and $R = 0.1218$ and $wR = 0.2750$ (all data). CCDC number: 740348.

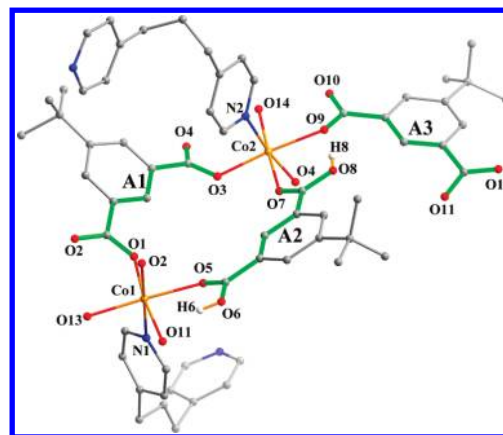


Figure 2. Portion of the view of **2** with atom labeling of the Co^{II} ions and O/N atoms in the asymmetric unit. The effective structural extension segments of the tbip and H_2tbip linkers are highlighted in green and nominated as A1, A2, and A3. Symmetry codes: A = $1/2 - x, 1/2 - y, -z$; B = $1 - x, y, 1/2 - z$.

carboxylate, one aqua ligand, and two bpp ligands, which each bridge to other Co2 atoms. This gives an overall 2D sheet structure (see Figures 1a and S3 in the Supporting Information).

Topologically, both $(\text{Co1})_2(\text{O}_2\text{C})_4$ dimers and discrete Co^{II} ions act as 4-connected nodes. The dimer nodes are connected to only Co2, whereas the Co2 nodes are directly connected to both dimer and other Co2 nodes. The resulting binodal 4-connected 2D net is quite unusual with a Schläfli symbol of $(4.6^4.8)_2(4^2.6^4)$, which may be properly regarded as two corrugated 2D 4⁴ layers that continually intersect at the shared dimeric Co^{II} nodes (see Figure 1b). Notably, this network consists of two different types of 4-connected nodes, with the vertex symbols of $(4.8_8.6_4.6_4.6_4.6_4)$ for Co2 and $(4.4.6_2.6_2.6_2.6_2)$ for the Co^{II} dimers, and a proportion of 2:1 in the overall 2D layer. Both the unidentate bpp ligands and the H-bonding interactions between the water ligands and uncoordinated carboxylate O atoms are ignored in the above topological discussion (although the unidentate bpp ligands are shown in black in Figure 1a). However, it is significant that the unidentate bpp ligands project through the rings created within the sheets by two bidentate bpp linkers and two pairs of H-bonding interactions, resulting in unusual rotaxane-like motifs. Each ring has one bpp rod passing through it, in opposite directions. Figure 1c displays the local environment with all of the non-H atoms and highlights the rotaxane-like interactions. Figure 1d shows a schematic view of the net in which the kinked nature of the bpp ligands is added, as the projecting unidentate terminals.

Complex **2** shows a 2D bilayer framework. In the asymmetric unit, there are two crystallographically independent Co^{II} centers, two tbip dianions, one H_2tbip molecule, a pair of half-bpp linkers, and two water ligands with half-occupancy (see Figure 2). The coordination spheres for the distorted octahedra Co1 and Co2 are quite similar and are composed of four O donors of three carboxylate and one carboxyl, one water ligand, and one pyridyl N atom of bpp. Each bpp ligand and aqua molecule, in turn, acts as a μ_2 -bridge to connect the Co^{II} centers. Notably, the dicarboxyl ligands have different degrees of deprotonation, and thus the binding fashions include two tbip dianions that are completely deprotonated with the di- μ_2 -O,O' and bi-monodentate modes and one neutral H_2tbip component that takes the bi-unidentate fashion.

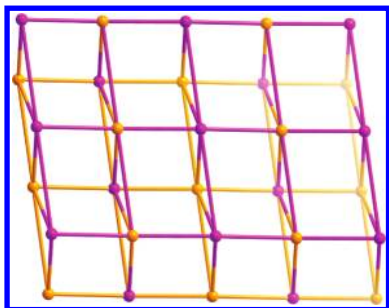


Figure 3. Schematic representation of the 6-connected topological net in **2**.

As a result, two independent dinuclear subunits formulated as $[\text{Co}_2(\mu\text{-COO})_2(\mu\text{-H}_2\text{O})]$ are formed, with adjacent $\text{Co1}\cdots\text{Co1}$ and $\text{Co2}\cdots\text{Co2}$ separations of 3.534 and 3.477 Å, respectively. Then, such dimers are further extended by the dicarboxyl and bpp ligands to afford a 2D bilayer network, in which the dimeric motifs are distributed alternately along the [100] and [010] axes (see Figure S4 in the Supporting Information). From the viewpoint of topology, by regarding each Co^{II} dimer as a net node, the coordination pattern of **2** can be described as a uninodal 6-connected network (see Figure 3) with the Schläfli symbol of $(3^3.4^{10}.5.6)$, which is completely different from the familiar 6-connected **hxl** layer (3^6 network). Notably, such a unique net can be realized by the zigzag linkages of two adjacent layers as subtectons and has only been found in the complex $\{[\text{Yb}(\text{L})_3](\text{CF}_3\text{SO}_3)_3\}_n$ (**L** refers to 4,4'-bipyridine-*N,N*-dioxide).^{9a} However, different styles of zigzag linkages are observed for both bilayer motifs (edge-to-edge for **2** and diagonal for the other case).

In order to gain a further understanding of the structural features of this interesting system, the roles of dicarboxyl and bpp tectons in framework assembly are analyzed as follows. Observably, only the effective structural extension segments of the dicarboxyl (see Figure 2 for details) and bpp ligands are present (that is to say, the irrelevant C and H atoms are omitted). As depicted in Figure 4, right, the octahedral Co^{II} centers are connected by two sets of bpp ligands, one set of A1-type tbip linkers, and one set of A2-type linkers (shown in the space-filling model) to result in a helical array along the [001] axis. Notably, four sets of helices are fused to each other by sharing of the metal centers to form an interconnected rod-shaped single bundle. In fact, the helical array thereof can be differentiated as $[-\text{N1}-\text{Co1}-\text{A1}-\text{Co2}-\text{N2}-\text{Co2}-\text{A1}-\text{Co1}-]_n$ (red, blue, and green lines, right-handed) and $[-\text{A2}-\text{Co1}-\text{O13}-\text{Co1}-\text{A2}-\text{Co2}-\text{O14}-\text{Co2}-]_n$ (space-filling section, left-handed), considering the involved coordination bonds. The pitch of the helix is 42.471 Å, being equal to 3 times the length of the *c* axis. As a result, the adjacent such rod-shaped bundles are further extended by the A3-type bridges to form the final 2D bilayer network (see Figure 4, left).

Thermogravimetric analysis (TGA; see Figure S5 in the Supporting Information) of **1** indicates that the first weight loss of 2.2% (calcd 2.0%) corresponds to the loss of one water molecule. The expulsion of organic components occurs from ca. 230 °C. The TGA curve for **2** shows the initial weight

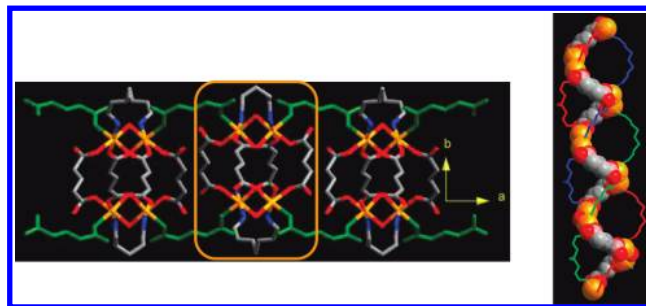


Figure 4. View of the 2D bilayer framework (left) of **2**, highlighting the interweaving of helices by sharing the same metal centers (right).

loss in the temperature range of 30–200 °C, which can be ascribed to the removal of one coordinated water molecule (obsd 1.9% and calcd 1.8%). Further heating indicates decomposition of the coordination framework.

The magnetic susceptibilities (χ_M) of **1** and **2** were measured in 2–300 K (see Figure S6 in the Supporting Information). As the temperature is reduced to 2 K, the $\chi_M T$ values continuously decrease, which indicates the antiferromagnetic interactions. The $\chi_M T$ values for **1** and **2** at room temperature are 5.61 and 4.92 $\text{cm}^3 \text{K mol}^{-1}$, respectively, being larger than that for two isolated Co^{II} ions (3.75 $\text{cm}^3 \text{K mol}^{-1}$). This value is a result of the contribution to the susceptibility from orbital angular momentum at higher temperatures. From the magnetic point of view, **1** and **2** can be regarded as a dinuclear model because coupling through mip, tbip, and bpp is almost negligible because of their long lengths. The susceptibility data were fit with an isotropic dimeric mode of the $S = 3/2$ spin, and the least-squares analysis gives $J = -7.1 \text{ cm}^{-1}$, $g = 2.35$, $zJ' = -0.74 \text{ cm}^{-1}$, and $R = 5.5 \times 10^{-4}$ for **1** and $J = -10.0 \text{ cm}^{-1}$, $g = 2.22$, $zJ' = -1.5 \text{ cm}^{-1}$, and $R = 9 \times 10^{-4}$ for **2**.

In summary, two unique 2D coordination polymers have been successfully synthesized by the hydrothermal route. The resulting network topologies are quite unusual and are constructed by different connections between two undulating 4^4 layers that can be regarded as the secondary building units. In addition, the unusual structural features of **1** and **2** with rotaxane and helix supramolecular motifs would promise them as intriguing members of 2D network-based crystalline materials.

Acknowledgment. We gratefully acknowledge financial support by the National Natural Science Foundation of China (Grants 20471026 and 20771054), Henan Tackle Key Problem of Science and Technology (Grants 072102270030 and 072102270034), Grant 2009GGJS-104, and the Foundation of Education Committee of Henan province (Grants 2006150017 and 2008A150018). M.D. also is thankful for support from Tianjin Normal University.

Supporting Information Available: Crystallographic data in CIF format, additional structural illustrations, PXRD patterns, TGA curves, and $\chi_M T/\chi_M$ vs T plots for complexes **1** and **2**. This material is available free of charge via the Internet at <http://pubs.acs.org>.